

# PHYSICAL REVIEW B

## CONDENSED MATTER

THIRD SERIES, VOLUME 55, NUMBER 21

1 JUNE 1997-I

### BRIEF REPORTS

*Brief Reports are accounts of completed research which, while meeting the usual Physical Review B standards of scientific quality, do not warrant regular articles. A Brief Report may be no longer than four printed pages and must be accompanied by an abstract. The same publication schedule as for regular articles is followed, and page proofs are sent to authors.*

#### ***In situ* neutron-reflectometry measurements of hydrogen and deuterium absorption in a Pd/Nb/Pd layered film**

Alan E. Munter and Brent J. Heuser

*Department of Nuclear Engineering, University of Illinois, 214 NEL, 103 South Goodwin Avenue, Urbana, Illinois 61801*

M. W. Ruckman

*Department of Physics, Brookhaven National Laboratory, Upton, New York 11973*

(Received 19 December 1996)

We present *in situ* neutron-reflectivity measurements of the hydrogen and deuterium absorption from the gas phase in a Pd/Nb/Pd thin film multilayer. Hydrogen and deuterium were both preferentially absorbed into the Nb layer at room temperature and at a pressure of 10 Torr. Genetic algorithm fits to the specular data indicate concentrations of approximately 0.71 [H]/[Nb] and 0.51 [D]/[Nb], placing the Nb well into the  $\beta$  phase (or an  $\alpha'$ -like phase). [S0163-1829(97)07021-5]

Many aspects of hydrogen in metals have been studied over the last several years.<sup>1,2</sup> Most studies of hydrogen in metals have been limited to bulk samples. With the growth of thin film fabrication technology, however, interest in the unique properties of thin film systems has increased. Physical properties of hydrogen-metal systems can be significantly altered by thin film geometries, and this has led to a fundamental interest beyond specific industrial applications.<sup>3</sup>

Several techniques have been applied to the study of the hydrogen content in metals: volumetric measurements,<sup>4</sup> resonant nuclear reaction analysis,<sup>5</sup> recoil reaction measurements,<sup>6,7</sup> x-ray diffraction,<sup>3,8</sup> nuclear magnetic resonance,<sup>9</sup> neutron scattering, and neutron reflectometry.<sup>10,11</sup> The majority of these methods do not provide depth distributions of hydrogen, however. The techniques most commonly used to study hydrogen profiles are resonant nuclear reaction analysis<sup>5</sup> and elastic recoil measurement.<sup>6</sup> These typically have resolutions of 50 to 100 Å.

As demonstrated in this work, neutron reflectometry can provide hydrogen depth distributions in thin films. As will be discussed in the following, hydrogen and deuterium will dramatically change the neutron-reflectivity response of a thin film. The present experiment was designed to demonstrate the sensitivity of neutron reflectivity to the preferential ab-

sorption of hydrogen and deuterium in a buried Nb film.

The film investigated here was a magnetron sputtered film on a flat glass substrate. The thin film was sputtered in 10 ppm purity argon gas at  $10^{-7}$  Torr. Starting from the substrate/film interface the approximate consistency of the film was 50 Å Cr, 450 Å Pd, 100 Å Nb, and 450 Å Pd. The Cr coating improved film adhesion under hydrogen and deuterium loading conditions. Hydrogen and deuterium solubility in Cr is very small, and the presence of this coating layer did not interfere with hydrogen and deuterium absorption in the Nb layer.

All reflectivity data were acquired at the Intense Pulsed Neutron Source at Argonne National Laboratory using the POSY II reflectometer.<sup>12</sup> POSY II utilizes a white beam of neutrons with wavelengths ranging from 2 to 16 Å emitted by a cold moderator consisting of solid methane at approximately 20 K. The scattered intensities are recorded as a function of time-of-flight by a one-dimensional, position sensitive detector. This detector measures both specular and off-specular events within the horizontal plane of reflection. Only specular events are considered here. The geometric angular resolution within the reflection plane  $\Delta\theta$  is approximately  $0.02^\circ$ . The detector accepts neutrons scattered out of the reflection plane by angles up to  $0.8^\circ$ , and all neutrons in this range are summed and treated as reflected neutrons

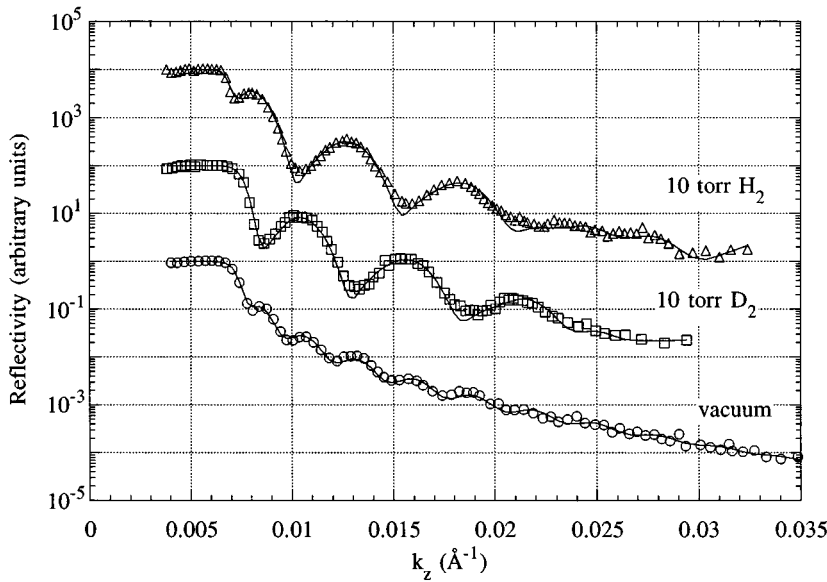


FIG. 1. Reflectivity curves for the Pd/Nb/Pd film before loading, loaded with deuterium, and loaded with hydrogen. Lines are best fits to the data.

within the reflection plane. For the measurements presented here, data sets were collected at two angles and merged together to get a full  $k_z$  range up to approximately  $0.03 \text{ \AA}^{-1}$ . The wave-vector transfer normal to the sample surface  $k_z$  is defined by

$$k_z = \frac{2\pi}{\lambda} \sin \theta, \quad (1)$$

where the angle between the sample surface and both the incident and reflected beams is given by  $\theta$  (for specular reflection), and  $\lambda$  is the neutron wavelength.

Most reflectivity curves have three basic features. The first is the critical wave-vector transfer  $k_c$ . Neutrons are totally reflected for values of  $k_z$  below  $k_c$ . For a uniform film,  $k_c$  is given by

$$k_c = 2\sqrt{\pi N b}, \quad (2)$$

where the scattering length density (SLD) is the product of the atomic number density  $N$  and the isotopically averaged, bound coherent neutron-scattering length  $b$ . Pd and Nb have nearly identical SLD values,  $4.01 \times 10^{-6} \text{ \AA}^{-2}$  and  $3.92 \times 10^{-6} \text{ \AA}^{-2}$ , respectively. For a nonuniform film the calculation is more complicated, but it is still a function of the average SLD of the film.

A second feature of reflectivity profiles is the decrease in intensity (or reflectivity) which, for a smooth sample, becomes proportional to  $k_z^{-4}$  as  $k_z$  increases. A thin film can also show oscillations, the third feature, around this continuously decreasing reflectivity; the result of an interference effect between the air/film and film/substrate interfaces. The amplitude of these thickness oscillations is proportional to the difference in SLD between the thin film and the substrate often referred to as the SLD contrast. An estimate of the film's thickness is given by  $\pi/\Delta k_z$ , where  $\Delta k_z$  is the oscillation period. As is the case here after hydrogen and deuterium loading the interference effect is altered when significant SLD contrast exists *within* the film.

The neutron-reflectivity response of the film was measured *in situ* using an environmental cell mounted on the

instrument. This cell could be evacuated, using an oil-free pumping system, down to  $10^{-3}$  Torr. All vacuum connections were grease free as well. The film was loaded by exposure to either 10 Torr of  $\text{H}_2$  and  $\text{D}_2$  gas.

Hydrogen and deuterium are often interchanged in neutron-scattering applications because they have chemically similar properties but very different scattering lengths. The bound atom coherent neutron scattering lengths are  $b_H = -3.7406 \times 10^{-13}$  and  $b_D = 6.671 \times 10^{-13}$  cm for the proton and deuterium, respectively. A film that absorbs hydrogen, therefore, will show the effects of a reduced SLD everywhere that hydrogen is present. The converse is true of a film that absorbs deuterium.

In all cases presented here, the reflectivity profiles were fit with a genetic algorithm<sup>13</sup> to determine the scattering length profile. This code calculates the neutron-reflectivity responses of a "family" of model profiles and compares these calculations to the measured data. The model with the best agreement is kept, a new "family" of profiles is generated. The process is repeated until the calculated neutron-reflectivity agrees with the measured data.

After the reflectivity measurements, the film was characterized with Auger electron spectroscopy (AES) to confirm the multilayer structure. This analysis was performed using a PHI 660 Auger electron spectrometer.

Figure 1 shows three reflectivity measurements recorded for the unloaded film, the hydrogen-loaded film, and the deuterium-loaded film. In the initial, unloaded, measurement little SLD contrast exists between the Pd and Nb layers and the total film thickness determines the oscillation period  $\Delta k_z$ . This simple analysis results in a film thickness of approximately  $1000 \text{ \AA}$ . Significant changes occur in the reflectivity response after deuterium and hydrogen loading as seen in Fig. 1. The oscillation period  $\Delta k_z$ , roughly doubles, indicating the film was split into two approximately equal halves. This is attributed to preferential absorption of hydrogen and deuterium by the center Nb layer creating a SLD gap. This hypothesis is confirmed by a calculation of the SLD profiles using the genetic algorithm procedure described above.

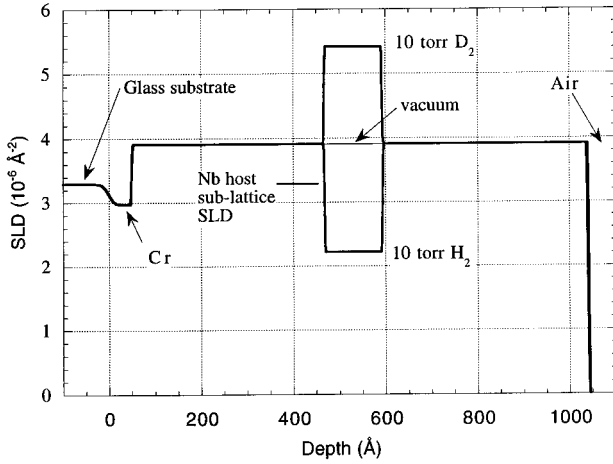


FIG. 2. The SLD profiles determined from fits to the data in Fig. 1 before loading, and loaded with hydrogen and deuterium.

Figure 2 shows SLD profiles obtained from fits to the three sets of neutron reflectivity data. The flat SLD profile is the unloaded film, while the profiles with deuterium and with hydrogen correspond to an increase and decrease in the niobium layer SLD, respectively. These profiles represent the simplest structure determinable from fits to the reflectivity data; the resolution of finer features requires an expansion of the  $k_z$  range with improved counting statistics.

To determine the concentration of hydrogen and deuterium absorbed by the Nb layer, the number density of the Nb sublattice is required. Although the Nb sublattice is known to expand anisotropically in the thin-film geometry (the in-plane constraining effect amplifies out-of-plane expansion),<sup>3</sup> a reasonable first-order approximation is to use the known expansion of the bulk  $\beta$  phase. The volumetric expansion within the two phase region is given by<sup>14</sup>

$$\frac{\Delta V}{V} = \frac{(1/N'_{\text{Nb}}) - (1/N_{\text{Nb}})}{(1/N_{\text{Nb}})} = 0.14C, \quad (3)$$

where  $C$  is the concentration of either hydrogen or deuterium,  $N_{\text{Nb}}$  is the atomic density of Nb before hydrogen or deuterium absorption, and  $N'_{\text{Nb}}$  is the atomic density after absorption. The right-hand side of Eq. (3) is based on the work of Peisl.<sup>14</sup> Using the measured SLD of the Nb layer

after hydrogen or deuterium absorption (Fig. 2) the following equations can be written:

$$N'_{\text{Nb}}b_{\text{Nb}} + N_{\text{H}}b_{\text{H}} = 2.22 \times 10^{-6} \text{ \AA}^{-2}, \quad (4a)$$

$$N'_{\text{Nb}}b_{\text{Nb}} + N_{\text{D}}b_{\text{D}} = 5.41 \times 10^{-6} \text{ \AA}^{-2}, \quad (4b)$$

where  $N_{\text{H}}$  and  $N_{\text{D}}$  are the atomic densities of hydrogen and deuterium in the Nb layer, respectively. Finally, realizing the concentration  $C$  in Eq. (3) is given by  $C = N_{\text{H}}/N'_{\text{Nb}}$  or  $N_{\text{D}}/N'_{\text{Nb}}$ , two sets of three equations can be solved for each concentration. The results of this calculation are  $[\text{H}]/[\text{Nb}] = 0.71$  and  $[\text{D}]/[\text{Nb}] = 0.51$ . The SLD of the as-loaded Nb sublattice is shown in Fig. 2 for comparison. The  $[\text{H}]/[\text{Nb}]$  and  $[\text{D}]/[\text{Nb}]$  ratios are consistent with the presence of a  $\beta$ -phase or a high concentration  $\alpha'$ -like phase.<sup>15</sup>

After the neutron-reflectivity measurements, the film was further characterized by AES. Figure 3 shows the concentration profiles measured as a function of sputtering time. The purpose of the AES measurement was to confirm the multilayer architecture and to check the film purity. Significant impurity levels beyond 1–2 % (the concentration limit of the instrument) were not observed. The profile also demonstrates that the deposition is symmetric about the midplane of the Nb layer (ignoring the Cr coating layer) so that the two Pd layers have approximately equal thicknesses.

Conversion of the profile given in Fig. 3 to a profile versus depth is not straightforward. First, the exact sputtering rates of Pd and Nb in the thin-film geometry are not known without the measurement of a thin-film standard. Second, ion bombardment broadens deeper interfaces because of longer exposure time. Finally, the difference in surface energies of Nb and Pd will result in intrinsically different interfacial widths for the Pd/Nb (Pd on top of Nb) and the Nb/Pd (Nb on top of Pd) interfaces.

These effects interfere with our ability to determine individual Pd and Nb layer thicknesses. However, using the total film thickness as given by the unloaded neutron-reflectivity measurement (approximately 990 Å), the following estimates can be made. First, we assume that the Pd to Nb sputtering rate ratio  $R_s$  ( $R_s \approx 2.94$  from the known bulk sputtering rates) is unaffected by the thin-film geometry. The ratio of Pd to Nb film thicknesses can then be determined from the ratio of sputtering times  $\alpha = \Delta t_{\text{Pd}}/\Delta t_{\text{Nb}}$ . The thickness of the individual Pd and Nb layers are given by

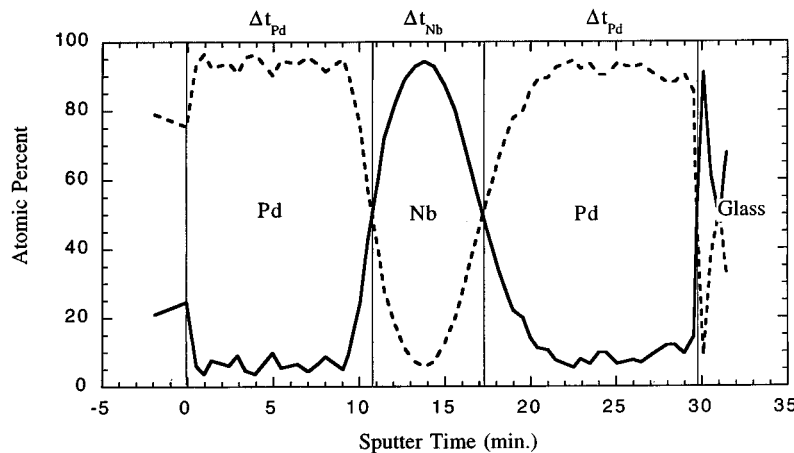


FIG. 3. Auger electron spectroscopy data from the Pd/Nb/Pd film.

$$T_{\text{Nb}} = \frac{(990 \text{ \AA})}{(1 + 2\alpha R_s)}, \quad (5a)$$

$$T_{\text{Pd}} = \frac{(990 \text{ \AA})\alpha R_s}{(1 + 2\alpha R_s)}. \quad (5b)$$

This analysis results in two 450-Å thick Pd layers and a 90-Å thick Nb layer. Although these thicknesses have perhaps 15–25 Å uncertainties, the 90-Å Nb layer thickness in the unloaded condition is consistent with the thickness of the Nb layer under hydrogen and deuterium absorption in Fig. 2.

This work was supported by the National Science Foundation under Grant No. DMR-9496297. Work at Brookhaven National Laboratory was supported by the U.S. DOE under Contract No. DE-AC02-76-CH00016 and BNL-CRADA No. C-94-03. Argonne National Laboratory is supported by the U.S. DOE, BES-Materials Sciences, under Contract No. W-31-109-ENG-38. The AES measurements were carried out at the Center for Microanalysis of Materials, University of Illinois, which is supported by the U.S. DOE under Grant No. DEFG02-91-ER45439. In addition, the help of Nancy Finnegan at the University of Illinois and Gideon Reisfeld (Elbit Corporation) are also acknowledged.

- 
- <sup>1</sup>G. Alefeld and J. Völkl, *Hydrogen in Metals I* (Springer, Berlin, 1978).
- <sup>2</sup>Y. Fukai, *The Metal-Hydrogen System* (Springer, Berlin, 1993).
- <sup>3</sup>P. F. Miceli, H. Zabel, J. A. Dura, and C. P. Flynn, *J. Mater. Res.* **6**, 964 (1991).
- <sup>4</sup>D. E. Azofeifa and N. Clark, *Z. Phys. Chem.* **181**, 387 (1993).
- <sup>5</sup>P. Trocellier and CH. Englemann, *J. Radiat. Nucl. Chem.* **100**, 117 (1986).
- <sup>6</sup>H. S. Cheng, Z. Y. Zhou, F. C. Yang, Z. W. Xu, and Y. H. Ren, *Nucl. Instrum. Methods Phys. Res.* **218**, 601 (1983).
- <sup>7</sup>G. G. Ross, B. Terreault, G. Gobeil, G. Abel, C. Boucher, and G. Veilleux, *J. Nucl. Mater.* **128-129**, 730 (1984).
- <sup>8</sup>Q. M. Yang, G. Schmitz, S. Fähler, H. U. Krebs, and R. Kirchheim, *Phys. Rev. B* **54**, 9131 (1996).
- <sup>9</sup>R. M. Cotts, *Ber. Bunsenges. Phys. Chem.* **76**, 760 (1972).
- <sup>10</sup>M. Mâaza, B. Farnoux, and F. Samuel, *Phys. Lett. A* **181**, 245 (1993).
- <sup>11</sup>C. F. Majkrzak, S. Satija, D. A. Neumann, J. J. Rush, D. Lashmore, C. Johnson, J. Bradshaw, L. Passell, and R. DiNardo, in *Neutron Scattering for Materials Science*, edited by S. M. Shapiro, S. C. Moss, and J. D. Jorgensen, MRS Symposia Proceedings No. 166 (Materials Research Society, Pittsburgh, 1990), p. 127.
- <sup>12</sup>A. Karim, B. H. Arendt, R. Goyette, Y. Y. Huang, R. Kleb, and G. P. Felcher, *Physica B* **173**, 17 (1991).
- <sup>13</sup>V. O. DeHaan and G. G. Drijckoning, *Physica B* **198**, 24 (1994).
- <sup>14</sup>H. Peisl, *Hydrogen in Metals I, Basic Properties*, Topics in Applied Physics (Springer-Verlag, Berlin, 1978), p. 53.
- <sup>15</sup>G. Reisfeld, M. M. Jisrawi, M. W. Ruckman, and M. Strongin, *Phys. Rev. B* **53**, 4974 (1996).